Available online at www.sciencedirect.com
SCIENCE DIRECT®
Journal of Solid State Chemistry 170 (2003) 106–117
JOURNAL OF SOLID STATE CHEMISTRY
http://elsevier.com/locate/jssc

Combinatorial topology of uranyl molybdate sheets: syntheses and crystal structures of $(C_6H_{14}N_2)_3[(UO_2)_5(MoO_4)_8](H_2O)_4$ and $(C_2H_{10}N_2)[(UO_2)(MoO_4)_2]$

Sergey V. Krivovichev[1] and Peter C. Burns*

Department of Civil Engineering and Geological Sciences, University of Notre Dame, 156 Fitzpatrick Hall, Notre Dame, IN 46556-0767, USA

Received 6 May 2002; received in revised form 23 July 2002; accepted 27 August 2002

Abstract

Two new mixed organic–inorganic uranyl molybdates, $(C_6H_{14}N_2)_3[(UO_2)_5(MoO_4)_8](H_2O)_4$ (**1**) and $(C_2H_{10}N_2)[(UO_2)(MoO_4)_2]$ (**2**), have been obtained by hydrothermal methods. The structure of **1** [triclinic, $P\bar{1}$, $Z=1$, $a=11.8557(9)$, $b=11.8702(9)$, $c=12.6746(9)$ Å, $\alpha=96.734(2)^\circ$, $\beta=91.107(2)^\circ$, $\gamma=110.193(2)^\circ$, $V=1659.1(2)$ Å] has been solved by direct methods and refined on the basis of F^2 for all unique reflections to $R1=0.058$, which was calculated for the 5642 unique observed reflections ($|F_o|\geqslant 4\sigma_F$). The structure contains topologically novel sheets of uranyl square bipyramids, uranyl pentagonal bipyramids, and MoO_4 tetrahedra, with composition $[(UO_2)_5(MoO_4)_8]^{6-}$, that are parallel to (-101). H_2O groups and 1,4-diazabicyclo [2.2.2]-octane (DABCO) molecules are located in the interlayer, where they provide linkage of the sheets. The structure of **2** [triclinic, $P\bar{1}$, $Z=2$, $a=8.4004(4)$, $b=11.2600(5)$, $c=13.1239(6)$ Å, $\alpha=86.112(1)^\circ$, $\beta=86.434(1)^\circ$, $\gamma=76.544(1)^\circ$, $V=1203.14(10)$ Å] has been solved by direct methods and refined on the basis of F^2 for all unique reflections to $R1=0.043$, which was calculated for 5491 unique observed reflections ($|F_o|\geqslant 4\sigma_F$). The structure contains topologically novel sheets of uranyl pentagonal bipyramids and MoO_4 tetrahedra, with composition $[(UO_2)(MoO_4)_2]^{2-}$, that are parallel to (110). Ethylenediamine molecules are located in the interlayer, where they provide linkage of the sheets. All known topologies of uranyl molybdate sheets of corner-sharing U and Mo polyhedra can be described by their nodal representations (representations as graphs in which U and Mo polyhedra are given as black and white vertices, respectively). Each topology can be derived from a simple black-and-white graph of six-connected black vertices and three-connected white vertices by deleting some of its segments and white vertices.

Keywords: Uranyl molybdates; Crystal structure; DABCO; Ethylenediamine

1. Introduction

The crystal chemistry of uranyl minerals and synthetic compounds has received considerable attention recently, owing to the importance of these phases in the environment [1]. They form in the oxidized portions of uranium deposits [2], in soils contaminated by actinides [3,4], are bio-precipitated by microbes intended for remediation of groundwater [5,6], are precipitated at reactive barriers intended to limit the mobility of U in groundwater [7,8], and are expected to form as alteration products of spent nuclear fuel and other nuclear waste forms in the proposed repository at Yucca Mountain, Nevada [9–13].

Uranyl molybdates are amongst the most structurally diverse of the uranyl compounds [14–22], with structural units including isolated uranyl molybdate clusters, chains, sheets and frameworks. Owing to the uneven distribution of bond strengths in uranyl polyhedra, infinite sheets are the most common structural unit in uranyl molybdates and uranyl compounds in general [23,24]. The topologies and geometries of uranyl molybdate sheets are strongly influenced by the size and electronic properties of cations located between the sheets. In addition to the numerous inorganic uranyl molybdate structures that have been reported recently, Halasayamani et al. [25] provided the structures of four

*Corresponding author. Fax: +1-574-631-9236.
E-mail address: pburns@nd.edu (P.C. Burns).
[1] Permanent address: Department of Crystallography, St. Petersburg State University, University Emb. 7/9. 199034 St. Petersburg, Russia.

0022-4596/03/$ - see front matter © 2002 Elsevier Science (USA). All rights reserved.
PII: S0022-4596(02)00033-6

mixed organic–inorganic uranyl molybdates, in which protonated organic molecules (templates) assume the role of complex interlayer cations that balance the charge of the uranyl molybdate sheet.

Here, we report the synthesis and crystal-structure determinations of two new organic–inorganic uranyl molybdates. Both contain novel sheets of uranyl and molybdate polyhedra. These structures provide insights into the combinatorial topology of layered uranyl molybdates. Previously, we developed a nodal approach for the description of uranyl molybdate units. Here, we show that all known topologies of sheets based upon corner-sharing U and Mo polyhedra can be derived from a simple net by deleting some of its segments and vertices.

2. Experimental

2.1. Syntheses

$(C_6H_{14}N_2)_3[(UO_2)_5(MoO_4)_8](H_2O)_4$: Crystals of $(C_6H_{14}N_2)_3[(UO_2)_5(MoO_4)_8](H_2O)_4$ (**1**) were obtained from a solution of $UO_2(CH_3COO)_2 \cdot 2H_2O$ (0.0784 g), MoO_3 (0.0576 g), 1,4-diazabicyclo[2.2.2]-octane (DABCO; 0.13 g) and HCl (0.035 g) in 5 ml of H_2O. The solution was placed in a Teflon-lined Parr bomb and heated to 180°C for 43 h, followed by cooling to ambient temperature. The crystals occur as aggregates of yellow transparent plates up to 0.2 mm in maximum dimension.

$(C_2H_{10}N_2)[(UO_2)(MoO_4)_2]$: Crystals of $(C_2H_{10}N_2)[(UO_2)(MoO_4)_2]$ (**2**) were obtained from a solution of $UO_2(CH_3COO)_2 \cdot 2H_2O$ (0.0784 g), MoO_3 (0.0576 g), ethylenediamine (0.03 g) and HCl (0.048 g) in 5 ml of H_2O. The solution was heated in a Teflon-lined Parr bomb to 180°C for 24 h, followed by cooling at 6°/h to ambient temperature. Greenish-yellow transparent platy crystals up to 0.3 mm in maximum dimension were recovered.

2.2. X-ray diffraction data collection

Crystals were mounted on a Bruker three-circle diffractometer equipped with a SMART APEX charge-coupled device (CCD) detector with a crystal-to-detector distance of 4.5 cm. Data were collected using monochromated Mo$K\alpha$ X-radiation with frame widths in ω of 0.3°. Unit-cell dimensions (Table 1) for **1** and **2** were refined using 3946 and 4228 reflections, respectively, and least-squares techniques. The three-dimensional data were reduced and filtered for statistical outliers using the Bruker program SAINT [26], and were corrected for Lorentz, polarization and background effects. Empirical absorption corrections for **1** and **2** were done on the basis of 598 and 684 reflections, respectively, by modeling the crystals as ellipsoids. This reduced R_{int} from 0.066 to 0.038 for **1**, and from 0.151 to 0.053 for **2**. Additional information pertinent to the data collections is given in Table 1.

Table 1
Crystallographic data and refinement parameters for $(C_6H_{14}N_2)_3[(UO_2)_5(MoO_4)_8](H_2O)_4$ (**1**) and $(C_2H_{10}N_2)[(UO_2)(MoO_4)_2]$ (**2**)

	1	**2**
a (Å)	11.8557(9)	8.4004(4)
b (Å)	11.8702(9)	11.2600(5)
c (Å)	12.6746(9)	13.1239(6)
α (deg)	96.734(2)	86.112(1)
β (deg)	91.107(2)	86.434(1)
γ (deg)	110.193(2)	76.544(1)
V (Å^3)	1659.1(2)	1203.14(10)
Space group	$P\bar{1}$	$P\bar{1}$
F_{000}	1348	1168
μ (cm^{-1})	136.99	155.24
Z	1	2
D_{calc} (g/cm^3)	3.02	3.60
Crystal size (mm)	$0.14 \times 0.04 \times 0.02$	$0.24 \times 0.08 \times 0.04$
Radiation	Mo$K\alpha$	Mo$K\alpha$
Total ref.	18 101	13 577
Unique ref.	12 883	9467
Unique $\lvert F_o\rvert \geq 4\sigma_F$	5642	5491
R_1	0.058	0.043
wR_2	0.136	0.078
S	0.820	0.700

Note: $R1 = \sum ||F_o| - |F_c|| / \sum |F_o|$;
$wR2 = \sum[w(F_o^2 - F_c^2)^2] / \sum[w(F_o^2)^2]^{1/2}$;
$w = 1/[\sigma^2(F_o^2) + (aP)^2 + bP]$, where $P = (F_o^2 + 2F_c^2)/3$;
$s = \sum[w(F_o^2 - F_c^2)]/(n-p)^{1/2}$, where n is the number of reflections and p is the number of refined parameters.

2.3. Structure solution and refinement

Scattering curves for neutral atoms, together with anomalous-dispersion corrections, were taken from International Tables for X-ray Crystallography, Vol. IV [27]. The Bruker SHELXTL Version 5 system of programs was used for the determination and refinement of the structure [28]. The structures of both **1** and **2** crystallize in space group $P\bar{1}$. The structure of **1** was solved by direct methods, which provided the positions of the U and Mo atoms. Anions were located on difference-Fourier maps calculated following refinement of the model. Two symmetrically independent DABCO molecules were identified and refined using isotropic approximations. During the course of refinement, we noted that the isotropic displacement parameters for the atoms of one of the DABCO molecules were approximately twice the size as the other. Therefore, the site occupancy factors for the atoms of this molecule were fixed at 0.5, which resulted in improvement of their U_{eq} parameters. The structure was refined on the basis of F^2 for all unique reflections, and converged to $R1 = 0.058$. The final model included anisotropic displacement parameters for U and Mo, as well as the O atoms bonded to U and Mo, and isotropic displacement

Table 2
Atomic coordinates and displacement parameters ($\times 10^4$ Å^2) for $(C_6H_{14}N_2)_3[(UO_2)_5(MoO_4)_8](H_2O)_4$ (**1**)

	x	y	z	U_{eq}	U_{11}	U_{22}	U_{33}	U_{23}	U_{13}	U_{12}
U(1)	0.58886(5)	0.28941(5)	0.09315(4)	165(1)	210(3)	112(3)	168(3)	−4(2)	−60(2)	60(2)
U(2)	0.0000	0.5000	0.5000	159(2)	209(4)	132(4)	133(4)	10(3)	−35(3)	61(3)
U(3)	0.16874(5)	0.14332(5)	0.70292(4)	179(1)	244(3)	135(3)	151(3)	1(2)	−84(2)	68(2)
Mo(1)	0.04842(12)	0.18656(11)	0.42796(10)	180(3)	243(7)	145(6)	141(6)	6(5)	−81(5)	62(5)
Mo(2)	0.67734(12)	0.99141(11)	0.07320(10)	192(3)	221(7)	130(6)	207(7)	9(5)	−115(5)	51(5)
Mo(3)	0.84598(12)	0.53048(11)	0.24357(10)	183(3)	272(7)	128(6)	136(6)	13(5)	−51(5)	59(5)
Mo(4)	0.56499(12)	0.59453(12)	0.12127(11)	216(3)	204(7)	224(7)	209(7)	52(5)	−64(5)	58(5)
O(1)	0.6923(10)	0.3165(10)	−0.0085(9)	270(30)	300(60)	290(60)	250(60)	70(50)	−40(50)	130(50)
O(2)	0.4853(10)	0.2547(10)	0.1922(9)	310(30)	350(70)	320(70)	280(70)	130(50)	−40(50)	100(50)
O(3)	0.0629(10)	0.1529(10)	0.7947(8)	280(30)	420(70)	290(60)	130(50)	30(50)	−100(50)	130(50)
O(4)	0.6541(11)	0.5014(10)	0.1384(10)	390(30)	530(80)	150(60)	490(80)	−140(50)	−260(60)	170(50)
O(5)	0.7989(10)	0.6459(9)	0.3081(8)	230(20)	310(60)	200(50)	170(50)	30(40)	−40(40)	100(50)
O(6)	0.2783(11)	0.1370(11)	0.6105(10)	370(30)	430(80)	350(70)	390(80)	40(60)	−100(60)	220(60)
O(7)	0.9105(11)	0.5677(10)	0.1276(8)	300(30)	490(80)	280(60)	140(50)	80(50)	−90(50)	120(50)
O(8)	0.9707(9)	0.5341(9)	0.3305(8)	230(20)	230(60)	280(60)	120(50)	−30(40)	−20(40)	30(50)
O(9)	0.1595(10)	0.5603(12)	0.4913(8)	350(30)	250(60)	580(80)	150(60)	−20(60)	−30(50)	100(60)
O(10)	0.0013(13)	0.3163(11)	0.4387(9)	390(30)	840(1 0 0)	320(70)	120(50)	40(50)	−30(60)	350(70)
O(11)	0.7448(9)	0.3754(9)	0.2338(8)	240(20)	270(60)	200(50)	260(60)	20(50)	−20(50)	110(50)
O(12)	0.0416(10)	0.1483(9)	0.5584(8)	250(20)	350(70)	260(60)	120(50)	−20(40)	−110(40)	120(50)
O(13)	0.6347(10)	0.1190(9)	0.1180(10)	340(30)	410(70)	140(50)	430(80)	−70(50)	−190(60)	90(50)
O(14)	0.5450(10)	0.8673(10)	0.0318(10)	350(30)	340(70)	180(60)	440(80)	−30(50)	−200(60)	20(50)
O(15)	−0.0557(13)	0.0590(10)	0.3502(9)	440(40)	830(1 0 0)	180(60)	190(60)	30(50)	−280(60)	10(60)
O(16)	0.7616(12)	0.0208(12)	−0.0365(10)	450(30)	560(90)	470(80)	300(70)	40(60)	50(60)	140(70)
O(17)	0.7562(10)	0.9664(10)	0.1802(9)	320(30)	300(60)	220(60)	370(70)	20(50)	−250(50)	40(50)
O(18)	0.5337(11)	0.6185(10)	−0.0119(9)	310(30)	410(70)	330(70)	300(70)	150(50)	−20(50)	210(60)
O(19)	0.6569(13)	0.7325(11)	0.1870(12)	590(50)	640(1 0 0)	240(70)	740(1 0 0)	0(70)	−610(80)	30(60)
O(20)	0.1996(11)	0.2201(14)	0.4046(11)	520(40)	250(70)	920(1 2 0)	430(80)	400(80)	40(60)	160(70)
O(21)	0.4392(12)	0.5552(14)	0.1922(10)	530(40)	410(80)	770(1 1 0)	290(80)	30(70)	20(60)	80(80)
H_2O(22)	0.4571(16)	0.5802(16)	0.5272(14)	820(50)						
H_2O(23)	0.6063(14)	0.2252(15)	−0.5846(13)	670(50)						
N(1)	0.0720(12)	0.2539(12)	0.2347(10)	260(30)						
N(2)	0.0924(14)	0.3157(14)	0.0431(12)	380(40)						
C(1)	−0.0498(15)	0.2582(15)	0.1930(14)	300(40)						
C(2)	0.1656(18)	0.3808(18)	0.2390(16)	440(50)						
C(3)	−0.0439(18)	0.2847(18)	0.0738(16)	430(50)						
C(4)	0.175(2)	0.428(3)	0.121(2)	770(80)						
C(5)	0.1124(19)	0.1636(19)	0.1615(17)	480(50)						
C(6)	0.140(2)	0.213(2)	0.0471(19)	610(60)						
N(3)[a]	0.6648(17)	0.1608(18)	−0.3928(16)	120(40)						
N(4)[a]	0.7230(17)	0.0816(17)	−0.2359(15)	40(40)						
C(7)[a]	0.792(2)	0.211(2)	−0.2268(19)	100(50)						
C(8)[a]	0.592(3)	0.060(3)	−0.243(2)	210(60)						
C(9)[a]	0.747(3)	0.019(3)	−0.330(2)	230(70)						
C(10)[a]	0.561(2)	0.107(3)	−0.333(2)	240(70)						
C(11)[a]	0.730(3)	0.258(3)	−0.311(2)	550(1 2 0)						
C(12)[a]	0.713(3)	0.069(3)	−0.428(2)	420(90)						

[a] s.o.f. = 0.5.

parameters for the H_2O groups and atoms of the DABCO molecules. Final atomic positional and displacement parameters are in Table 2, and selected interatomic distances are in Table 3.

The structure of **2** was solved by direct methods, which provided the positions of the U and Mo atoms. Difference-Fourier maps calculated following refinement of the model provided the remaining atomic positions. Anisotropic displacement parameters were refined for all non-hydrogen atoms, and the positional parameters of 20 H atoms were included in the refinement. The isotropic displacement parameters for the H atoms were constrained to be equal; the C–H and N–H bond lengths were constrained to be ~1.10 and ~1.00 Å, respectively. Final atomic positional and displacement parameters are in Table 4, and selected interatomic distances are in Table 5. Tables of observed and calculated structure factors for both structures are available from the authors upon request.

Table 3
Selected bond lengths (Å) and angles (deg) in the structure of $(C_6H_{14}N_2)_3[(UO_2)_5(MoO_4)_8](H_2O)_4$ (**1**)

U(1)–O(2)	1.76(1)	Mo(2)–O(16)f	1.73(1)
U(1)–O(1)	1.78(1)	Mo(2)–O(17)	1.74(1)
U(1)–O(13)	2.32(1)	Mo(2)–O(14)	1.76(1)
U(1)–O(4)	2.36(1)	Mo(2)–O(13)f	1.79(1)
U(1)–O(14)a	2.38(1)	⟨Mo(2)–O⟩	1.76
U(1)–O(18)a	2.38(1)		
U(1)–O(11)	2.41(1)	Mo(3)–O(7)	1.70(1)
⟨U(1)–O_{Ur}⟩	1.77	Mo(3)–O(5)	1.77(1)
⟨U(1)–O_{eq}⟩	2.37	Mo(3)–O(11)	1.81(1)
		Mo(3)–O(8)	1.81(1)
U(2)–O(9),b	1.79(1) 2×	⟨Mo(3)–O⟩	1.77
U(2)–O(10),b	2.23(1) 2×		
U(2)–O(8)c,d	2.28(1) 2×	Mo(4)–O(21)	1.71(1)
⟨U(2)–O_{Ur}⟩	1.79	Mo(4)–O(19)	1.73(1)
⟨U(2)–O_{eq}⟩	2.26	Mo(4)–O(18)	1.80(1)
		Mo(4)–O(4)	1.80(1)
U(3)–O(3)	1.75(1)	⟨Mo(4)–O⟩	1.76
U(3)–O(6)	1.78(1)		
U(3)–O(15)e	2.32(1)	Mo(4)–O(4)–U(1)	125.6(6)
U(3)–O(12)	2.37(1)	Mo(3)–O(5)–U(3)d	137.8(6)
U(3)–O(19)d	2.39(1)	Mo(3)–O(8)–U(2)g	137.5(5)
U(3)–O(5)d	2.42(1)	Mo(1)–O(10)–U(2)	158.0(7)
U(3)–O(17)d	2.43(1)	Mo(3)–O(11)–U(1)	121.6(5)
⟨U(3)–O_{Ur}⟩	1.77	Mo(1)–O(12)–U(3)	140.8(6)
⟨U(3)–O_{eq}⟩	2.39	Mo(2)h–O(13)–U(1)	153.5(7)
		Mo(2)–O(14)–U(1)a	154.9(7)
Mo(1)–O(20)	1.74(1)	Mo(1)–O(15)–U(3)e	158.2(6)
Mo(1)–O(15)	1.76(1)	Mo(2)–O(17)–U(3)d	159.0(6)
Mo(1)–O(12)	1.76(1)	Mo(4)–O(18)–U(1)a	135.8(6)
Mo(1)–O(10)	1.80(1)	Mo(4)–O(19)–U(3)d	151.9(7)
⟨Mo(1)–O⟩	1.77		
N(1)···O(20)	2.75(2)	$a = -x+1, -y+1, -z; b = -x, -y+1, -z+1;$	
N(2)···O(7)	2.71(2)	$c = x-1, y, z; d = -x+1, -y+1, -z+1;$	
N(3)···H_2O(23)	2.78(3)	$e = -x, -y, -z+1; f = x, y+1, z;$	
N(4)···O(16)	2.78(2)	$g = x+1, y, z; h = x, y-1, z.$	
H_2O(22)–H_2O(22)d	2.49(3)		
H_2O(22)–H_2O(23)a	2.69(2)		

3. Results

3.1. Cation coordination polyhedra

$(C_6H_{14}N_2)_3[(UO_2)_5(MoO_4)_8](H_2O)_4$: The structure of **1** contains three symmetrically distinct U^{6+} cations, each of which are strongly bonded to two O atoms, forming approximately linear $(UO_2)^{2+}$ uranyl ions (Ur) with U–O_{Ur} bond lengths of ~1.8 Å. Two of the uranyl ions are coordinated by five O atoms arranged at the equatorial vertices of pentagonal bipyramids that are capped by the O_{Ur} atoms, with ⟨U–O_{eq}⟩ bond lengths (eq: equatorial) of 2.37 and 2.39 Å for U(1) and U(3), respectively. The third uranyl ion is coordinated by only four O atoms, giving a square bipyramid, with a ⟨U–O_{eq}⟩ bond length of 2.29 Å. Although this coordination polyhedron is relatively common in uranyl compounds [23], **1** is the first uranyl molybdate that contains both uranyl square and pentagonal bipyramids. The ⟨U–O_{eq}⟩ bond lengths in all three uranyl polyhedra are in excellent agreement with the average ⟨U–O_{eq}⟩ bond lengths of 2.37(9) and 2.28(5) Å for uranyl pentagonal and square bipyramids, respectively, derived from numerous well-refined structures [23]. The U(2) site is on an inversion center, which is common in uranyl molybdates with UrO_4 square bipyramids [17–19].

Four symmetrically independent Mo^{6+} cations are tetrahedrally coordinated by O atoms. The ⟨Mo–O⟩ bond lengths in the MoO_4 tetrahedra range from 1.76 to 1.77 Å. Individual bonds to O atoms that bridge between molybdate and uranyl polyhedra range from 1.73 to 1.81 Å, whereas bonds to terminal O atoms are in the range 1.70–1.74 Å.

Bond–valence sums for the atoms in the structure of **1** were calculated using parameters given by Burns et al. [23] for U^{6+}–O bonds and by Brese and O'Keeffe [29] for Mo^{6+}–O bonds. The bond–valence sums are 6.08, 6.22, 6.03, 5.89, 6.04, 5.80 and 5.99 v.u. (valence units)

Table 4
Atomic coordinates and displacement parameters ($\times 10^4$ Å^2) for $(C_2H_{10}N_2)[(UO_2)(MoO_4)_2]$ (**2**)

	x	y	z	U_{eq}	U_{11}	U_{22}	U_{33}	U_{23}	U_{13}	U_{12}
U(1)	0.76415(4)	0.72692(3)	0.12706(2)	135(1)	163(2)	119(2)	116(1)	−22(1)	−6(1)	−17(1)
U(2)	0.26564(4)	0.22641(3)	0.37462(2)	136(1)	166(2)	119(2)	114(1)	−17(1)	−14(1)	−9(1)
Mo(1)	0.25473(9)	0.42122(6)	0.59478(5)	159(2)	207(4)	139(3)	129(3)	−21(3)	−11(3)	−31(3)
Mo(2)	0.24432(9)	0.08203(6)	0.11460(5)	163(2)	215(4)	135(3)	135(3)	−14(3)	−19(3)	−26(3)
Mo(3)	0.37672(9)	0.05258(6)	0.64477(5)	147(2)	204(4)	94(3)	124(3)	−21(2)	−6(3)	6(3)
Mo(4)	0.13093(9)	0.44919(6)	0.13264(5)	148(2)	192(4)	106(3)	130(3)	−14(2)	−20(3)	0(3)
O(1)	0.9501(7)	0.7745(5)	0.1238(4)	225(14)	290(40)	170(30)	230(30)	−60(20)	−20(30)	−70(30)
O(2)	0.5807(7)	0.6754(6)	0.1311(5)	244(14)	250(40)	230(30)	270(30)	−80(30)	−40(30)	−60(30)
O(3)	0.4555(8)	0.2681(6)	0.3663(5)	263(15)	320(40)	190(30)	280(30)	−80(30)	−20(30)	−30(30)
O(4)	0.2844(8)	−0.0744(6)	0.1427(5)	276(15)	420(40)	160(30)	240(30)	60(30)	−100(30)	−50(30)
O(5)	0.0786(8)	0.1793(6)	0.3824(5)	268(15)	290(40)	260(40)	280(30)	−60(30)	20(30)	−100(30)
O(6)	0.2095(9)	0.5792(6)	0.6072(5)	323(17)	500(50)	110(30)	350(40)	−20(30)	−80(30)	−20(30)
O(7)	−0.0758(7)	0.5214(5)	0.1132(4)	201(13)	160(30)	100(30)	320(30)	−50(20)	0(30)	20(20)
O(8)	0.3292(7)	0.1069(5)	−0.0101(4)	204(13)	280(30)	190(30)	120(30)	0(20)	−30(20)	0(30)
O(9)	0.5824(7)	−0.0173(5)	0.6075(4)	183(12)	160(30)	110(30)	260(30)	0(20)	40(20)	−10(20)
O(10)	0.3285(7)	0.1498(5)	0.2111(4)	206(13)	320(40)	150(30)	160(30)	−30(20)	50(30)	−80(30)
O(11)	0.2517(7)	0.5563(6)	0.1160(5)	273(15)	180(30)	250(40)	390(40)	−10(30)	−10(30)	−50(30)
O(12)	0.1718(7)	0.3563(6)	0.7083(4)	216(13)	250(30)	250(30)	170(30)	20(20)	−10(30)	−120(30)
O(13)	0.1731(7)	0.3932(5)	0.4792(4)	222(14)	360(40)	170(30)	100(30)	−50(20)	−10(30)	50(30)
O(14)	0.2588(7)	−0.0542(6)	0.6513(5)	282(15)	220(40)	220(40)	410(40)	−110(30)	30(30)	−50(30)
O(15)	0.2007(8)	0.3300(5)	0.0476(4)	230(14)	350(40)	190(30)	100(30)	−20(20)	60(30)	10(30)
O(16)	0.3669(8)	0.1205(6)	0.7634(4)	281(15)	410(40)	240(40)	150(30)	−80(30)	0(30)	20(30)
O(17)	0.1495(8)	0.3851(6)	0.2581(4)	275(15)	380(40)	210(30)	170(30)	−20(30)	0(30)	80(30)
O(18)	0.0330(7)	0.1347(6)	0.1177(5)	303(16)	220(30)	400(40)	300(40)	−10(30)	−70(30)	−80(30)
O(19)	0.4689(7)	0.3693(6)	0.5913(5)	305(16)	150(30)	350(40)	400(40)	−90(30)	−80(30)	10(30)
O(20)	0.2979(8)	0.1663(6)	0.5524(5)	298(16)	390(40)	240(40)	200(30)	30(30)	−50(30)	60(30)
N(1)	0.2186(10)	0.7268(8)	0.7646(6)	280(19)	390(50)	260(50)	210(40)	−60(30)	−40(40)	−110(40)
N(2)	0.2534(10)	0.7873(7)	0.4924(6)	230(17)	330(50)	240(40)	160(40)	−−40(30)	0(30)	−130(40)
N(3)	0.2983(11)	−0.2872(8)	0.2668(6)	274(18)	350(50)	320(50)	170(40)	−60(30)	40(40)	−120(40)
N(4)	−0.2456(11)	0.2269(8)	0.0087(6)	284(19)	410(50)	240(50)	220(40)	−20(30)	−30(40)	−100(40)
C(1)	0.6556(13)	0.3390(10)	0.1660(7)	310(20)	330(60)	360(60)	210(50)	−50(40)	40(40)	0(50)
C(2)	−0.1455(12)	0.1628(10)	0.5913(7)	290(20)	250(50)	330(60)	280(50)	−10(40)	20(40)	−50(40)
C(3)	0.6195(13)	0.2552(11)	0.0886(7)	340(20)	310(60)	490(70)	230(50)	50(50)	−10(40)	−140(50)
C(4)	−0.1459(15)	0.2610(12)	0.6661(9)	470(30)	510(80)	580(80)	380(70)	0(60)	−250(60)	−230(60)

Hydrogen positions[a]

H(1)	−0.041(8)	0.207(8)	0.709(7)	H(11)	0.230(13)	0.858(6)	0.538(6)
H(2)	−0.230(13)	0.300(6)	−0.035(7)	H(12)	0.214(12)	0.717(6)	0.525(7)
H(3)	0.607(12)	0.170(5)	0.127(7)	H(13)	0.677(12)	0.412(7)	0.111(6)
H(4)	0.275(11)	0.786(8)	0.727(7)	H(14)	0.541(10)	0.322(7)	0.037(6)
H(5)	0.388(9)	−0.327(9)	0.312(7)	H(15)	0.297(12)	−0.355(6)	0.223(6)
H(6)	0.558(8)	0.383(9)	0.220(6)	H(16)	−0.204(11)	0.088(6)	0.612(7)
H(7)	−0.018(5)	0.146(9)	0.559(7)	H(17)	0.113(7)	0.784(8)	0.783(8)
H(8)	0.299(13)	−0.205(5)	0.233(7)	H(18)	0.197(12)	0.683(8)	0.704(5)
H(9)	−0.135(6)	0.179(8)	0.025(8)	H(19)	0.372(4)	0.774(10)	0.506(8)
H(10)	−0.332(9)	0.205(9)	−0.030(7)	H(20)	−0.131(12)	0.348(5)	0.629(7)

[a] $U_{eq} = 0.0490(70)$ Å^2 for all hydrogen positions (restrained to be equal during refinement).

for the U(1), U(2), U(3), Mo(1), Mo(2), Mo(3) and Mo(4) atoms, respectively. Sums at the O atom positions range from 1.57 to 2.12 v.u.; the lowest sums correspond to terminal O atoms of the MoO_4 tetrahedra [O(20): 1.57 v.u.; O(16): 1.61 v.u.; O(21): 1.70 v.u.; O(7): 1.75 v.u.], which probably accept H bonds from the H_2O groups and the DABCO molecules (see below).

$(C_2H_{10}N_2)[(UO_2)(MoO_4)_2]$: The structure of **2** contains two symmetrically distinct U^{6+} cations, both of which are in uranyl pentagonal bipyramidal coordination polyhedra. The $\langle U–O_{Ur}\rangle$ and $\langle U–O_{eq}\rangle$ bond distances are 1.76 and 2.37 Å, respectively, for both of the U(1) and U(2) sites. There are four independent Mo^{6+} cations, each of which is coordinated by four atoms of O, with $\langle Mo–O\rangle$ bond lengths ranging from 1.75 to 1.77 Å. As in **1**, the Mo–O bonds to the terminal O atoms are shorter, in the range 1.722–1.756 Å, than those to bridging O atoms, which are in the range of 1.745–1.789 Å.

Bond valences incident upon the atomic positions were calculated as for **1** above. Bond–valence sums are

Table 5
Selected bond lengths (Å) and angles (deg) in the structure of $(C_2H_{10}N_2)[(UO_2)(MoO_4)_2]$ (**2**)

U(1)–O(1)	1.762(6)	N(1)–C(1)a	1.47(1)
U(1)–O(2)	1.765(6)	N(2)–C(2)f	1.46(1)
U(1)–O(12)a	2.339(5)	N(3)–C(4)g	1.49(2)
U(1)–O(16)a	2.343(6)	N(4)–C(3)e	1.49(1)
U(1)–O(8)b	2.356(5)	C(1)–C(3)	1.52(1)
U(1)–O(7)c	2.403(5)	C(2)–C(4)	1.53(2)
U(1)–O(15)b	2.404(5)	N(1)···O(14)	2.87(1)
⟨U(1)–O_{Ur}⟩	1.76	N(1)···O(18)	2.77(1)
⟨U(1)–O_{eq}⟩	2.37	N(1)···O(6)	2.75(1)
		N(2)···O(14)	2.84(1)
U(2)–O(3)	1.760(6)	N(2)···O(6)	2.78(1)
U(2)–O(5)	1.766(6)	N(2)···O(19)	2.79(1)
U(2)–O(17)	2.343(6)	N(2)···O(3)	3.08(1)
U(2)–O(10)	2.351(6)	N(3)···O(19)	2.74(1)
U(2)–O(13)	2.357(6)	N(3)···O(4)	2.79(1)
U(2)–O(20)	2.398(6)	N(3)···O(11)	2.84(1)
U(2)–O(9)d	2.406(5)	N(4)···O(11)	2.84(1)
⟨U(2)–O_{Ur}⟩	1.76	N(4)···O(18)	2.77(1)
⟨U(2)–O_{eq}⟩	2.37	N(4)···O(4)	2.80(1)
Mo(1)–O(6)	1.747(6)	Mo(4)–O(7)–U(1)e	134.1(3)
Mo(1)–O(19)	1.756(6)	Mo(2)–O(8)–U(1)b	126.9(3)
Mo(1)–O(13)	1.779(5)	Mo(3)–O(9)–U(2)d	131.2(3)
Mo(1)–O(12)	1.789(6)	Mo(2)–O(10)–U(2)	141.7(3)
⟨Mo(1)–O⟩	1.77	Mo(1)–O(12)–U(1)a	143.0(3)
		Mo(1)–O(13)–U(2)	128.2(3)
Mo(2)–O(4)	1.733(6)	Mo(4)–O(15)–U(1)b	146.7(3)
Mo(2)–O(18)	1.735(6)	Mo(3)–O(16)–U(1)a	149.1(3)
Mo(2)–O(8)	1.775(6)	Mo(4)–O(17)–U(2)	150.4(3)
Mo(2)–O(10)	1.784(6)	Mo(3)–O(20)–U(2)	148.0(4)
⟨Mo(2)–O⟩	1.76		
Mo(3)–O(14)	1.722(6)		
Mo(3)–O(20)	1.745(6)		
Mo(3)–O(16)	1.770(6)		
Mo(3)–O(9)	1.777(6)	$a = -x+1, -y+1, -z+1$;	
⟨Mo(3)–O⟩	1.75	$b = -x+1, -y+1, -z; c = x+1, y, z$;	
Mo(4)–O(11)	1.743(6)	$d = -x+1, -y, -z+1; e = x-1, y, z$;	
Mo(4)–O(17)	1.753(6)	$f = -x, -y+1, -z+1; g = -x, -y, -z+1$.	
Mo(4)–O(7)	1.764(5)		
Mo(4)–O(15)	1.774(6)		
⟨Mo(4)–O⟩	1.76		

6.12, 6.12, 5.83, 6.01, 6.07 and 5.98 v.u. for the U(1), U(2), Mo(1), Mo(2), Mo(3) and Mo(4) atoms, respectively. The bond–valence sums for the O atoms are in the range of 1.50–2.08 v.u.; the lowest sums correspond to terminal O atoms of the MoO_4 tetrahedra, which presumably accept H bonds from the protonated ethylenediamine molecules.

3.2. Structural connectivity and hydrogen bonding

$(C_6H_{14}N_2)_3[(UO_2)_5(MoO_4)_8](H_2O)_4$: The structure of **1** contains sheets of uranyl square and pentagonal bipyramids and MoO_4 tetrahedra, with composition $[(UO_2)_5(MoO_4)_8]^{6-}$ (Figs. 1a and 2). The polyhedra are linked by the sharing of equatorial vertices of uranyl polyhedra with molybdate tetrahedra (Fig. 2). The Mo–O–U bond angles range considerably, from 121.6 to 159.0°, reflecting the flexible nature of the interpolyhedral linkages, in agreement with observations for other uranyl molybdates [20]. The $[(UO_2)_5(MoO_4)_8]^{6-}$ sheets are parallel to (−101), with H_2O groups and DABCO molecules located between the sheets, where they provide linkage of the sheets into a three-dimensional structure via hydrogen bonds (Fig. 1a).

We were unable to locate the H atom positions for **1** in the difference-Fourier maps. It is possible to propose some H bonds on the basis of N···O interatomic distances. There is a single O atom or H_2O group located from 2.7 to 2.8 Å from each of the four

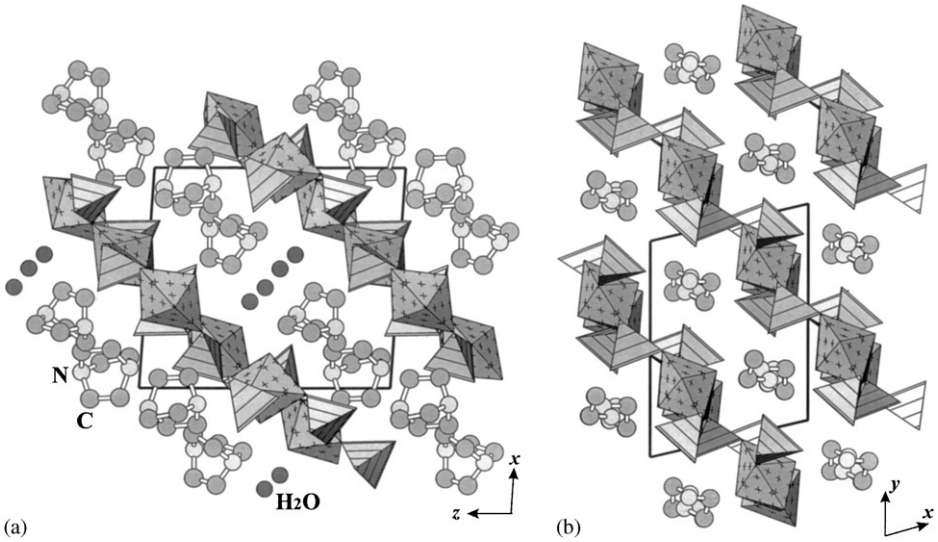

Fig. 1. (a) The structure of $(C_6H_{14}N_2)_3[(UO_2)_5(MoO_4)_8](H_2O)_4$ (**1**) viewed along the *b*-axis; (b) the structure of $(C_2H_{10}N_2)[(UO_2)(MoO_4)_2]$ (**2**) viewed along the *c*-axis. U polyhedra are cross-hatched; Mo polyhedra are shaded with parallel lines.

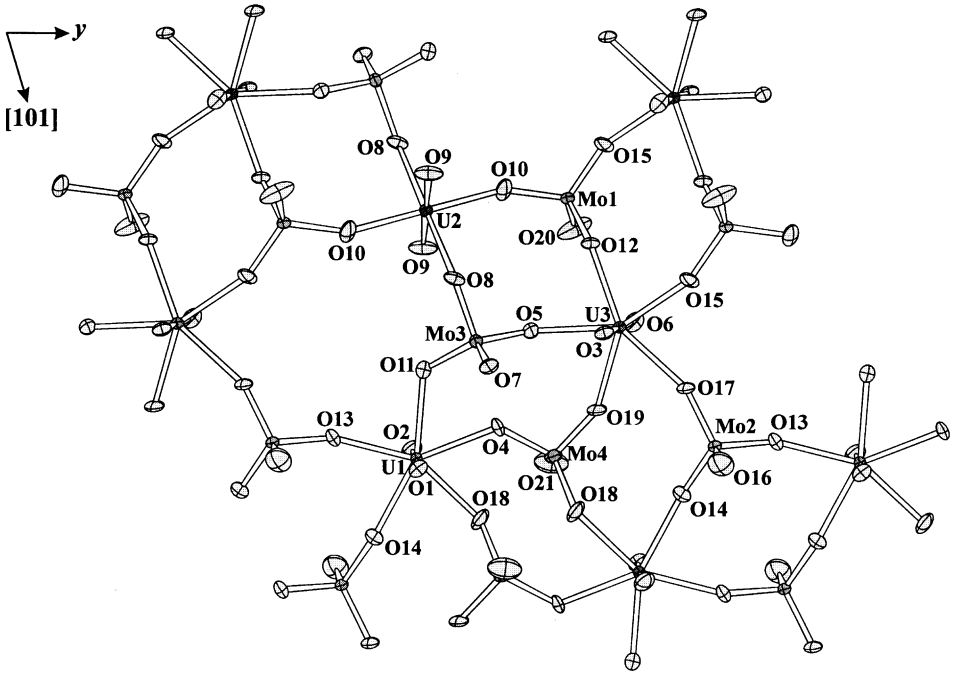

Fig. 2. The $[(UO_2)_5(MoO_4)_8]^{6-}$ sheet in the structure of $(C_6H_{14}N_2)_3[(UO_2)_5(MoO_4)_8](H_2O)_4$ (**1**) (ellipsoids are drawn at the 50% probability level).

symmetrically independent N atoms (Table 3). These distances are appropriate for N–H···O hydrogen bonds.

$(C_2H_{10}N_2)[(UO_2)(MoO_4)_2]$: The structure of **2** contains sheets of corner-sharing UrO_5 pentagonal bipyramids and MoO_4 tetrahedra, with composition $[(UO_2)(MoO_4)_2]^{2-}$ (Figs. 1b and 3), that are parallel to (110). Numerous uranyl dimolybdate compounds are known that involve uranyl molybdate sheets; nevertheless, the sheet found in **2** is novel. Two symmetrically independent $[C_2H_{10}N_2]^{2+}$ molecules are located in the interlayer and link adjacent sheets into a three-dimensional structure. It was possible to locate all H atoms in the difference-Fourier maps (Table 4). Most of the N atoms are involved in moderate N–H···O bonds that are accepted by terminal O atoms of MoO_4 tetrahedra (Fig. 4) [O(4), O(6), O(8), O(11), O(14), O(18), O(19)]. The corresponding N···O and H···O distances range from 2.74 to 2.87 and 1.77 to 2.12 Å, respectively. The N–H···O angles are in the range of 124–168°. The N(2) atom probably forms a bifurcated N–H(12)···O bond to the O(3) atom of the $(U(2)O_2)^{2+}$ ion and the O(19) atom. The corresponding NO and H···O distances are in the range 2.79–3.08 and 2.24–2.25 Å, respectively.

4. Discussion

4.1. Topology of the uranyl molybdate sheets

The topological relations amongst uranyl molybdate sheets may be examined using nodal representations or sheet anion-topologies. In the case of nodal representations, each node represents either a UrO_n bipyramid ($n = 4$ or 5; black circle) or a MoO_4 tetrahedron (white circle). Nodes are connected if the corresponding polyhedra share at least one common vertex. Each connecting line corresponds to an anion that is shared between the polyhedra. Thus, each uranyl molybdate structural unit has a corresponding black-and-white graph that represents the topology of the polyhedral linkage.

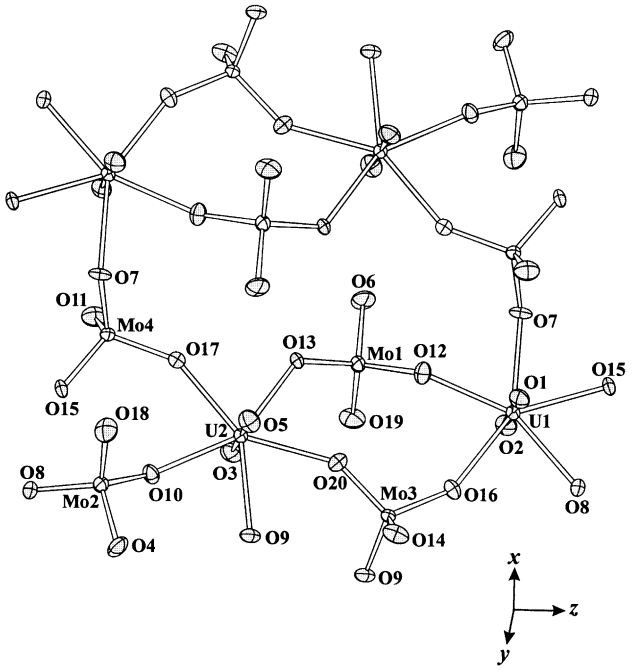

Fig. 3. The $[(UO_2)(MoO_4)_2]^{2-}$ sheet in the structure of $(C_2H_{10}N_2)[(UO_2)(MoO_4)_2]$ (**2**) (ellipsoids are drawn at the 50% probability level).

The topological structure of uranyl molybdate sheets may be examined on the basis of sheet anion-topologies, which were developed by Burns et al. [24,30] for the classification and comparison of sheets in uranyl minerals and synthetic inorganic compounds in general. In the development of an anion-topology, all cations are removed from consideration, whereas anions in the plane of the sheet that are separated by less than ~ 3.5 Å are joined by lines. Projection of the sheet anion-topology provides a two-dimensional tiling of space that ideally reflects the packing of anions within the plane of the sheet.

Polyhedral representations of the $[(UO_2)_5(MoO_4)_8]^{6-}$ and $[(UO_2)(MoO_4)_2]^{2-}$ sheets found in **1** and **2**, together with their corresponding graphs and sheet anion-topologies, are given in Figs. 5 and 6, respectively. The anion-topology of the $[(UO_2)_5(MoO_4)_8]^{6-}$ sheet (Fig. 5e) consists of hexagons, pentagons, squares and triangles. The corresponding sheet has all hexagons empty, the pentagons are populated by U(1) and U(3), one-fourth of the squares contain U(2), and two-thirds of the triangles are populated by Mo, such that a face of the MoO_4 tetrahedron corresponds to the triangle. The anion-topology of the $[(UO_2)(MoO_4)_2]^{2-}$ sheet consists of pentagons and triangles. In the corresponding sheet, one-third of the pentagons and one-quarter of the triangles are populated by U and Mo atoms, respectively. The sheet anion-topologies corresponding to the structures of **1** and **2** are reported here for the first time [24,30].

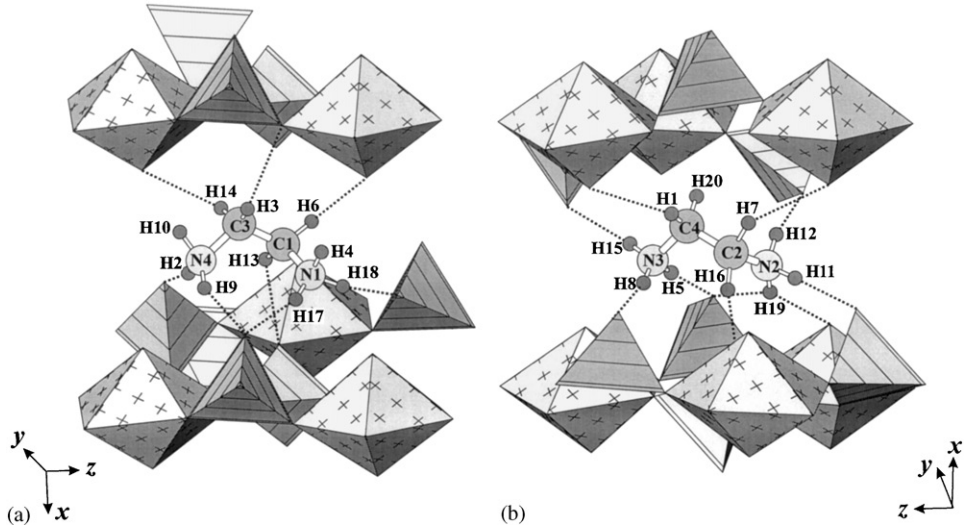

Fig. 4. Hydrogen bonding associated with the two symmetrically independent ($C_2H_{10}N_2$) molecules in the structure of $(C_2H_{10}N_2)[(UO_2)(MoO_4)_2]$ (**2**). H···O bonds are shown as dashed lines. The legend is as in Fig. 1.

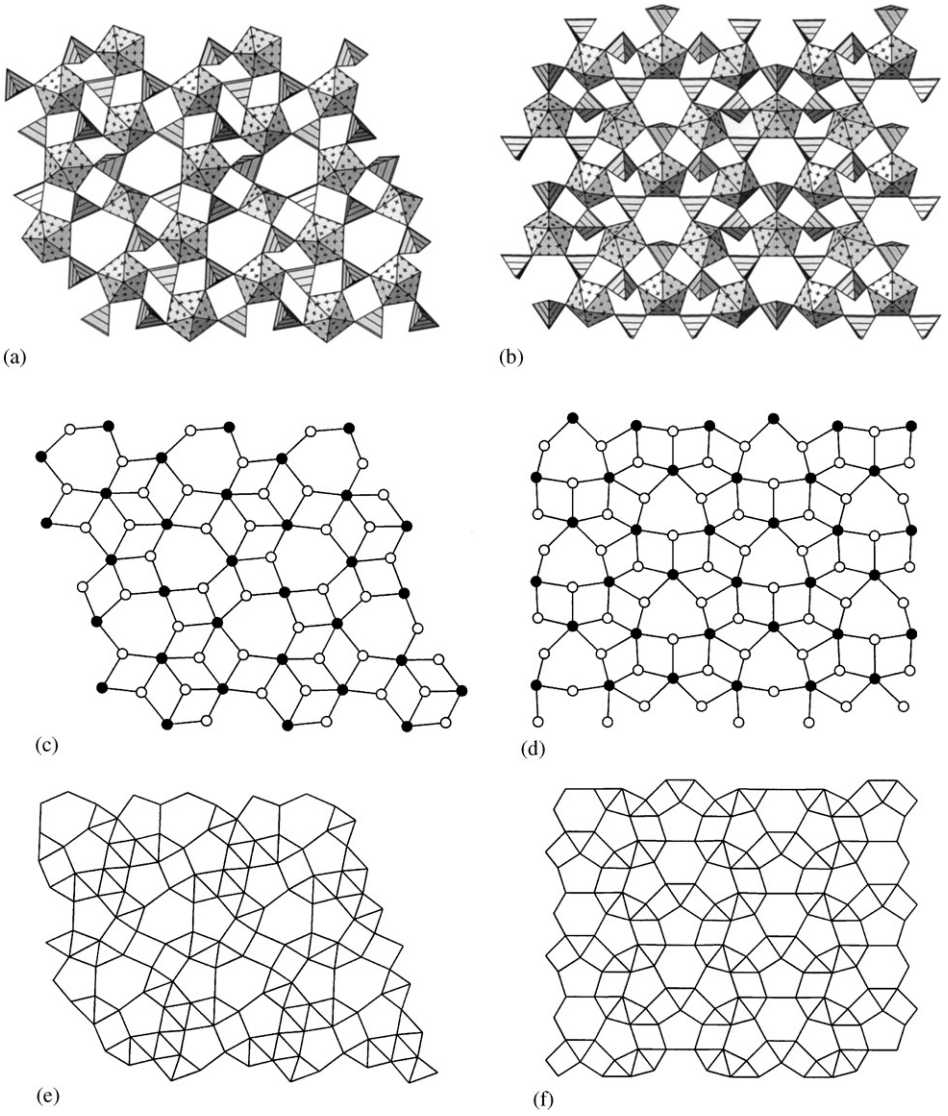

Fig. 5. The $[(UO_2)_5(MoO_4)_8]^{6-}$ and $[(UO_2)_3(MoO_4)_5]^{4-}$ sheets from the structures of $(C_6H_{14}N_2)_3[(UO_2)_5(MoO_4)_8](H_2O)_4$ (**1**) and $(NH_3(CH_2)_3NH_3)(H_3O)_2[(UO_2)_3(MoO_4)_5]$ [25]: (a) and (b) their polyhedral representations, respectively; (c) and (d) their nodal representations, respectively (U = black; Mo = white); (e) and (f) their anion-topologies, respectively. See text for details.

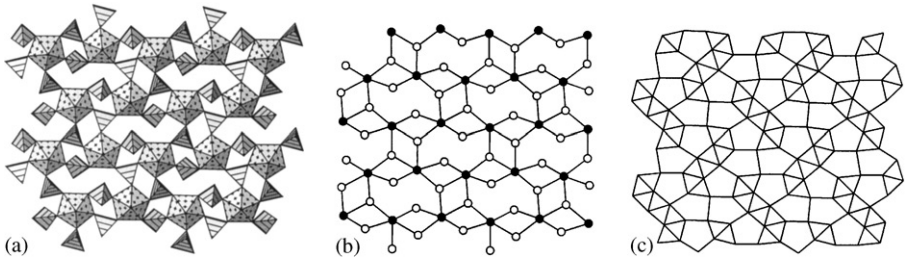

Fig. 6. The $[(UO_2)(MoO_4)_2]^{2-}$ sheet from the structure of $(C_2H_{10}N_2)[(UO_2)(MoO_4)_2]$ (**2**): (a) its polyhedral representation; (b) its nodal representation (U = black; Mo = white); (c) its anion-topology.

4.2. Topologies of uranyl molybdate sheets built by corner-sharing U and Mo coordination polyhedra

Five topologically distinct uranyl molybdate sheets are known that involve corner-sharing of U coordination polyhedra and MoO_4 tetrahedra. Using a graphical approach, the topology of each sheet can be derived from the simple black-and-white graph shown in Fig. 7a. In this graph, each white node is three-connected and each black vertex is six-connected. In

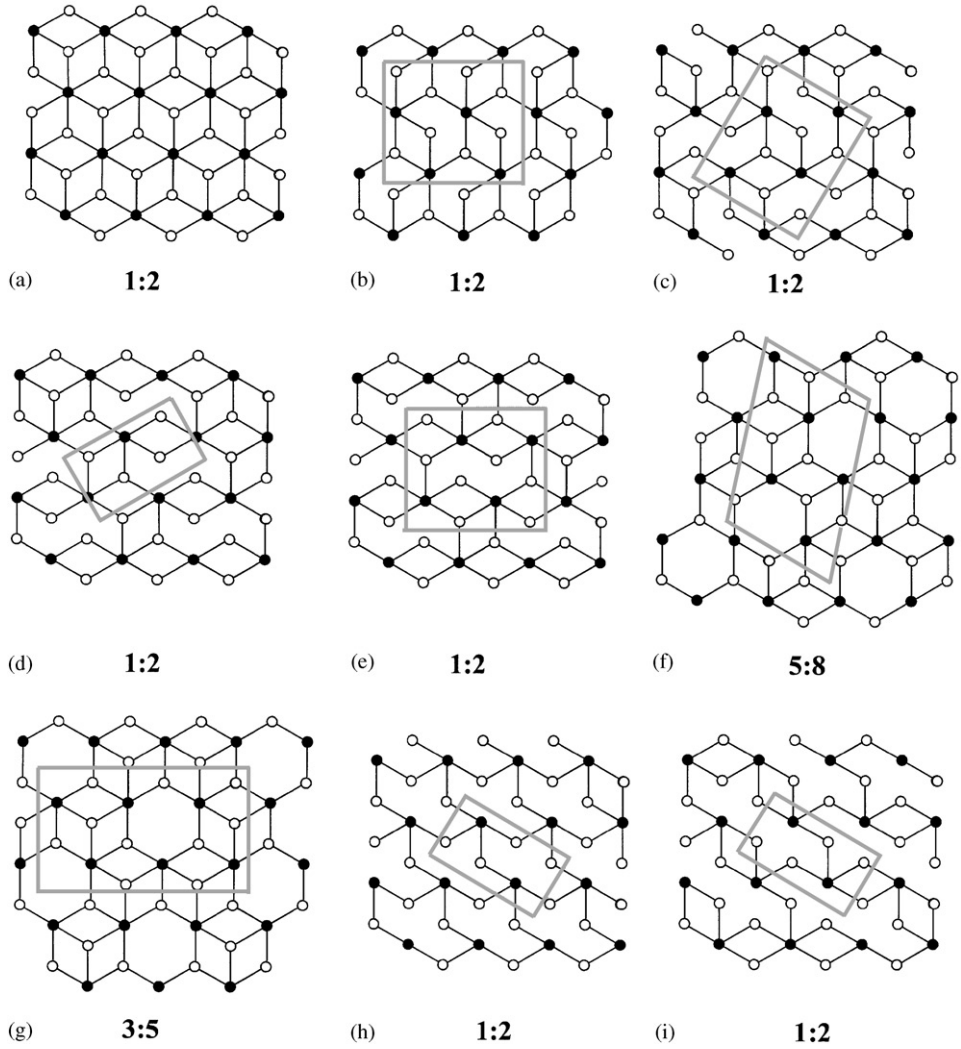

Fig. 7. The ideal graph of six-connected black and three-connected white vertices (a) and its derivatives (b–i). The graphs shown in (b–f) corresponds to observed topologies of U (black vertices) and Mo (white vertices) polyhedral linkages in uranyl molybdate sheets. See text for details.

crystal chemical terms, this corresponds to the case where all U polyhedra (black vertices) are hexagonal bipyramids that share all six equatorial corners with MoO_4 tetrahedra. Although such a sheet is theoretically possible, it has not been observed. In all known uranyl molybdate sheets, the U^{6+} cations form UrO_5 pentagonal bipyramids or UrO_4 square bipyramids. Thus, modification of the graph shown in Fig. 7a to correspond to known structures involves elimination of one or two segments around each black vertex. Note that the U:Mo ratio for the graph shown in Fig. 7a is 1:2. Elimination of segments from the graph does not change this ratio; the only condition we impose is that each black vertex is either five- or four-connected, whereas white vertices can be two- or three-connected. Three graphs can be obtained from the full graph (Fig. 7a) that correspond to observed uranyl molybdate sheets.

The graph shown in Fig. 7b corresponds to the $[(UO_2)(MoO_4)_2]^{2-}$ sheet observed in the structures of $M(UO_2)_3(MoO_4)_4(H_2O)_8$ (M = Mg, Zn) [31] and $M_2[(UO_2)(MoO_4)_2](H_2O)$ (M = NH_4, Rb, Cs) [17,21]. In the structures of $M(UO_2)_3(MoO_4)_4(H_2O)_8$ (M = Mg, Zn), these sheets are linked by additional $UrO_4(H_2O)$ bipyramids, resulting in a framework. In $M_2[(UO_2)(MoO_4)_2](H_2O)$ (M = NH_4, Rb, Cs), two sheets are linked, forming a double sheet, which is further linked by additional $UrO_4(H_2O)$ bipyramids, resulting in a framework.

The graph shown in Fig. 7c corresponds to the $[(UO_2)(MoO_4)_2]^{2-}$ sheet in the structures of a large number of uranyl dimolybdates: $M_2[(UO_2)(MoO_4)_2]$ (M = K, Rb, Cs, Tl) [21,22,32], $M_2[(UO_2)(MoO_4)_2](H_2O)$ (M = NH_4, K, Rb, Cs) [18,33–35] and $(C_5H_{14}N_2)[(UO_2)(MoO_4)_2](H_2O)$ [25]. The $[(UO_2)(MoO_4)_2]^{2-}$ sheet of this topology is very flexible, which

presumably relates to its abundance in uranyl molybdates. A $[(UO_2)(SeO_3)_2]^{4-}$ sheet with the same topology occurs in the structures of $M[(UO_2)(HSeO_3)(SeO_3)]$ ($M = NH_4$, K, Rb, Cs, Tl) [36,37] and $(NH_4)_2[(UO_2)(SeO_3)_2](H_2O)_{0.5}$ [38].

The graph shown in Fig. 7d corresponds to the $[(UO_2)(MoO_4)_2]^{2-}$ sheet found in the structures of $Na_2[(UO_2)(MoO_4)_2]$ [18] and $(C_4H_{12}N_2)[(UO_2)(MoO_4)_2]$ [25]. Sheets of composition $[(NpO_2)(MoO_4)_2]^{3-}$ and $[(UO_2)(SeO_3)_2]^{4-}$ with this topology occur in $K_3[(NpO_2)(MoO_4)_2$ [39] and $Ag_2[(UO_2)(SeO_3)_2]$ [37], respectively.

The graph shown in Fig. 7e is a distorted version of the graph shown in Fig. 6b, and corresponds to the $[(UO_2)(MoO_4)_2]^{2-}$ sheet found in $(C_2H_{10}N_2)[(UO_2)(MoO_4)_2]$. Remarkably, this graph is not equivalent in a combinatorial sense with any of the 1:2 graphs shown in Figs. 7b–d.

The graphs shown in Figs. 7b–e can be obtained from that in Fig. 7a by simply eliminating segments joining black and white vertices. In contrast, the two graphs depicted in Figs. 7f and g can be obtained only by deletion of selected white vertices. This operation changes the U:Mo ratio from 1:2 to 1:n, where n is less than 2. The resulting graphs (Figs. 7f and g) contain six-membered rings of alternating black and white vertices. The graph shown in Fig. 7f has a black:white ratio of 5:8 (= 1:1.60) and corresponds to the $[(UO_2)_5(MoO_4)_8]^{6-}$ sheet observed in the structure of **1** (this work). The graph shown in Fig. 7g has a black:white ratio of 3:5 (= 1:1.67) and corresponds to the $[(UO_2)_3(MoO_4)_5]^{4-}$ sheet from the structure of $(NH_3(CH_2)_3NH_3)(H_3O)_2[(UO_2)_3(MoO_4)_5]$ [25]. These sheets are closely related, and they are compared in more detail in Fig. 5. The major topological difference between the sheets is the existence of four-connected black vertices in the graph corresponding to the $[(UO_2)_5(MoO_4)_8]^{6-}$ sheet (Fig. 5e). The anion-topologies for the two sheets (Figs. 5e and f) have some features in common, although they are not identical. Both topologies contain hexagons due to the existence of six-membered rings of U and Mo polyhedra. In the anion-topology of the $[(UO_2)_5(MoO_4)_8]^{6-}$ sheet (Fig. 5e), the hexagons share three of their six edges with two pentagons and a square, which are all populated by U in the corresponding sheet, whereas, in the $[(UO_2)_3(MoO_4)_5]^{4-}$ sheet, the hexagons share edges with three pentagons that are populated by U in the corresponding sheet (Fig. 5f).

It is noted that the graphical approach developed here can be applied to several sheets involving corner-sharing of UrO_5 pentagonal bipyramids and SO_4 tetrahedra. For example, the graph shown in Fig. 7h corresponds to the $[(UO_2)(SO_4)_2(H_2O)]^{2-}$ sheet found in the structures of $[(UO_2(SO_4)_2(H_2O)](C(NH_2)_3)_2)(H_2O)_2$ [40], $H_2[(UO_2)(SO_4)_2(H_2O)](H_2O)_4$ [41], $Mg[(UO_2)(SO_4)_2(H_2O)](H_2O)_{10}$ [42] and $K_2[(UO_2)(SO_4)_2(H_2O)](H_2O)$ [43]. The graph shown in Fig. 7i corresponds to the $[(UO_2)(SO_4)_2(H_2O)]^{2-}$ sheet found in $(NH_4)_2[(UO_2)(SO_4)_2(H_2O)](H_2O)$ [44].

5. Conclusions

We have shown that representation of uranyl molybdate sheets as graphs is a powerful tool for comparison of their topological structures, and for establishing topological relationships between different structures. This approach can also be applied to other uranyl compounds that are based on sheets of corner-sharing cation polyhedra, especially those containing tetrahedral, pseudotetrahedral (as selenite) or triangular anions. Comparison of the graphs shown in Figs. 5c and d with those shown in Figs. 7f and g, respectively, shows that "embedding" these graphs into real space requires distortion of the ideal structure due to the interactions of the sheet with interlayer species. This distortion can be described in terms of cooperative motions of relatively rigid U and Mo polyhedra that will be the subject of a forthcoming paper.

Acknowledgments

This research was supported by the Environmental Management Sciences Program of the United States Department of Energy (Grant DE-FG07-97ER 14820) and by the Russian Foundation for Basic Research for S.V.K. (Grant 01-05-64883).

References

[1] P.C. Burns, R.J. Finch (Eds.), Uranium: mineralogy, geochemistry and the environment, Reviews in Mineralogy, Vol. 38, Mineralogical Society of America, Washington, DC, 1999.
[2] C. Frondel, Systematic mineralogy of uranium and thorium, US Geological Survey Bulletin 1064 (1958) 1.
[3] E.C. Buck, N.R. Brown, N.L. Deitz, Environ. Sci. Technol. 30 (1996) 81–88.
[4] Y. Roh, S.Y. Lee, M.P. Elless, K.S. Cho, J. Environ. Sci. Health A 35 (2000) 1043–1059.
[5] L.E. Macaskie, K.M. Bonthrone, P. Yong, D.T. Goddard, Microbiol.-UK 146 (2000) 1855–1867.
[6] G. Basnakova, J.A. Finlay, L.E. Macaskie, Biotechnol. Lett. 20 (1998) 949–952.
[7] C.C. Fuller, J.R. Barger, Abstracts of Papers of the American Chemical Society, Vol. 222, 2001, 41-GEOC.
[8] C.C. Fuller, J.R. Barger, J.A. Davis, M.J. Piana, Environ. Sci. Technol. 36 (2002) 158–165.
[9] D.J. Wronkiewicz, J.K. Bates, T.J. Gerding, E. Veleckis, B.S. Tani, J. Nucl. Mater. 190 (1992) 107–127.
[10] D.J. Wronkiewicz, J.K. Bates, S.F. Wolf, E.C. Buck, J. Nucl. Mater. 238 (1996) 78.
[11] P.A. Finn, J.C. Hoh, S.F. Wolf, S.A. Slater, J.K. Bates, Radiochim. Acta 74 (1996) 65–71.

[12] R.J. Finch, E.C. Buck, P.A. Finn, J.K. Bates, in: D.J. Wronkiewicz, J. H. Lee (Eds.), Scientific Basis for Nuclear Waste Management XXII, Boston, Vol. 556, Materials Research Society Symposium Proceedings, 1999, pp. 431–438.
[13] P.C. Burns, R.A. Olson, R.J. Finch, J.M. Hanchar, Y. Thibault, J. Nucl. Mater. 278 (2000) 290–300.
[14] S.V. Krivovichev, P.C. Burns, Can. Mineral. 38 (2000) 717.
[15] S.V. Krivovichev, P.C. Burns, Can. Mineral. 38 (2000) 847.
[16] S.V. Krivovichev, P.C. Burns, Can. Mineral. 39 (2001) 197.
[17] S.V. Krivovichev, P.C. Burns, Can. Mineral. 39 (2001) 207.
[18] S.V. Krivovichev, R.J. Finch, P.C. Burns, Can. Mineral. 40 (2002) 193.
[19] S.V. Krivovichev, P.C. Burns, Can. Mineral. 40 (2002) 201.
[20] S.V. Krivovichev, C.L. Cahill, P.C. Burns, Inorg. Chem. 41 (2002) 34.
[21] S.V. Krivovichev, P.C. Burns, J. Solid State Chem. (in press).
[22] S.V. Krivovichev, P.C. Burns, manuscript in preparation.
[23] P.C. Burns, F.C. Hawthorne, R.C. Ewing, Can. Mineral. 35 (1997) 1551.
[24] P.C. Burns, M.L. Miller, R.C. Ewing, Can. Mineral. 34 (1996) 845.
[25] P.S. Halasayamani, R.J. Francis, S.M. Walker, D. O'Hare, Inorg. Chem. 38 (1999) 271.
[26] SAINT, V5.01 Program for Reduction of Data Collected on Bruker AXS CCD Area Detector Systems, Bruker Analytical X-ray Systems, Madison, WI, 1998.
[27] J.A. Ibers, W.C. Hamilton (Eds.), International Tables for X-ray Crystallography, Vol. IV, The Kynoch Press, Birmingham, UK, 1974.
[28] SHELXTL NT, V5.1 Program Suite for Solution and Refinement of Crystal Structures, Bruker Analytical X-ray Systems, Madison, WI, 1998.
[29] N.E. Brese, M. O'Keeffe, Acta Crystallogr. B 47 (1991) 192.
[30] P.C. Burns, Rev. Mineral. 38 (1999) 23.
[31] V.V. Tabachenko, V.V. Kovba, V.N. Serezhkin, Koord. Khim. 9 (1983) 1568.
[32] G.G. Sadikov, T.I. Krasovskaya, Yu.A. Polyakov, V.P. Nikolaev, Izv. AN SSSR, Neorg. Mater. 24 (1988) 109.
[33] R.K. Rastsvetaeva, A.V. Barinova, A.M. Fedoseev, N.A. Budantseva, Yu.V. Nekrasov, Dokl. Akad. Nauk 365 (1999) 68.
[34] V.N. Khrustalev, G.B. Andreev, M.Yu. Antipin, A.M. Fedoseev, N.A. Budantseva, I.B. Shirokova, Zh. Neorg. Khim. 45 (2000) 1996.
[35] G.B. Andreev, M.Yu. Antipin, A.M. Fedoseev, N.A. Budantseva, Koord. Khim. 27 (2001) 227.
[36] M. Koskenlinna, J. Valkonen, Acta Crystallogr. C 52 (1996) 1857.
[37] P.M. Almond, T.E. Albrecht-Schmitt, Inorg. Chem. 41 (2002) 1177.
[38] M. Koskenlinna, I. Mutikainen, T. Leskela, M. Leskela, Acta Chem. Scand. 51 (1997) 264.
[39] M.S. Grigoriev, I.A. Charushnikova, A.M. Fedoseev, N.A. Budantseva, A.I. Yanovskii, Yu.T. Struchkov, Radiokhimiya 34 (5) (1992) 7.
[40] R.F. Baggio, A.R. De Benyacar, B.O. Perazzo, P.K. De Perazzo, Acta Crystallogr. B 33 (1977) 3495.
[41] N.W. Alcock, M.M. Roberts, D. Brown, J. Chem. Soc. Dalton Trans. 1982 (1982) 869.
[42] V.N. Serezhkin, M.A. Soldatkina, V.A. Efremov, Zh. Strukt. Khim. 22 (1981) 174.
[43] L. Niinistoe, J. Toivonen, J. Valkonen, Acta Chem. Scand. A 33 (1979) 621.
[44] L. Niinistoe, J. Toivonen, J. Valkonen, Acta Chem. Scand. A 32 (1978) 647.